TRANSNAV International Journal on Marine Navigation and Safety of Sea Transportation
Volume 5 Number 4 December 2011

Surface Reflection and Local Environmental Effects in Maritime and other Mobile Satellite Communications

S. D. Ilcev
Durban University of Technology (DUT), Durban, South Africa

ABSTRACT: This paper introduces the effects of surface reflections and local environmental as very important particulars for mobile and especially for Maritime Satellite Communications (MSC), because such factors generally tend to impair the performance of satellite communications links, although signal enhancements are also occasionally observed. Local environmental effects include shadowing and blockage from objects and vegetation near the Ship Earth Station (SES) and other mobile terminals. The advantages and disadvantages of those effects are discussed, the areas of surface reflection were examined and the further investigations of local environmental are provided. At this point, surface reflections are generated either in the immediate vicinity of the SES terminals or from distant reflectors, such as mountains and large industrial infrastructures. Specific issues related to these challenges are concluded and a set of solutions is proposed to maximize the availability of satellite communication capacity to the mobile user applications. The specific effects on propagation in the mobile environments are examined and explained important characteristics of the Interference from Adjacent Satellite Systems, Specific Local Environmental Influence in MSC, different Noise Contribution of Local Ships' Environment, Blockages Caused by Ship Superstructures and Motion of Ship's Antenna.

1 INTRODUCTION

The reflected transmission signal can interfere with the direct signal from the satellite to produce unacceptable levels of signal degradation. In addition to fading, signal degradations can include intersymbol interference, arising from delayed replicas. The impact of the impairments depends on the specific application, namely in the case of typical Land MSC (LMSC) links, all measurements and theoretical analysis indicate that the specular reflection component is usually negligible for path elevation angles above 20o.

Moreover, for handheld terminals, specular reflections may be important as the low antenna directivity increases the potential for significant specular reflection effects. For Maritime MSC (MMSC), LMSC and Aeronautical MSC (AMSC) system links, design reflection multipath fading, in combination with possible shadowing and blockage of the direct signal from the satellite, is generally the dominant system impairment.

2 REFLECTION FROM THE EARTH'S SURFACE

Prediction of the propagation impairments caused by reflections from the Earth's surface and from different objects (buildings, hills, vegetation) on the surface is difficult because the possible impairment scenarios are quite numerous, complex and often cannot be easily quantified. For example, the degree of shadowing in LMSC satellite links frequently cannot be precisely specified.

Therefore, impairment prediction models for some complicated situations, especially for LMSC links, tend to be primarily empirical, while more analytical models, such as those used to predict sea reflection fading, have restricted regions of applicability. Nevertheless, the basic features of surface reflections and the resultant effects on propagating signals can be understood in terms of the general theory of surface reflections, as summarized in the following classification:

1 Specular Reflection from a Plane Earth – Here, this effect is less than or equal to the coefficient for horizontal polarization. Thus the polarization of the reflected waves will be different from the polarization of the incident wave if the incident

polarization is not purely horizontal or purely vertical. For example, a circularly polarized incident wave becomes elliptically polarized after reflection.

2 Specular Reflection from a Smooth Spherical Earth – Here, the incident grazing angle is equal to the angle of reflection. The amplitude of the reflected signal is equal to the amplitude of the incident signal multiplied by the modules of the reflection coefficient.

3 Divergence Factor – When rays are secularly reflected from a spherical surface, there is an effective reduction in the reflection coefficient, which is a geometrical effect arising from the divergence of the rays.

4 Reflection from Rough Surface – In many practical cases, the surface of the Earth is not smooth. Namely, when the surface is rough, the reflected signal has two components: one is a specular component, which is coherent with the incident signal, while the other is a diffuse component, which fluctuates in amplitude and phase with a Rayleigh distribution.

5 Total Reflected Field – The total field above a reflecting surface is a result of the direct field, the coherent specular component and the random diffuse component.

6 Reflection Multipath – Owing to the existence of surface reflection phenomena signals may arrive at a receiver from multiple apparent sources. Thus, the combination of the direct signal (line-of-sight) with specular and diffusely reflected waves causes signal fading at the receiver. The resultant multipath fading, in combination with varying levels of shadowing and blockage of the line-of-sight components, can cause the received signal power to fade severely and rapidly for MES and is really the dominant impairment in the Global Mobile Satellite Communications (GMSC) service.

3 FADING IN MMSC AND AMSC SYSTEMS DUE TO SEA SURFACE REFLECTION

Multipath fading due to sea reflection is caused by interference between direct and reflected radiowaves. The reflected radiowaves are composed of coherent and incoherent components, namely specular and diffuse reflections, respectively, that fluctuate with time due to the motion of sea waves. The coherent component is predominant under calm sea conditions and at low elevation angles, whereas the incoherent becomes significant in rough sea conditions. If the intensity of the coherent component and the variance of the incoherent component are both known, the cumulative time distribution of the signal intensity can be determined by statistical consideration.

In any event, a prediction model for multipath fading due to sea reflection, however, was first developed for MMSC systems at a frequency near 1.5 GHz. Although the mechanism of sea reflection is common for MMSC and AMSC systems, only with the difference that fading characteristics for AMSC are expected to differ from those for MMSC, this is because the speed and altitude of aircraft so much greater than those of ships. At this point, the effects of refractions and scattering by the sea surface become quite severe in case of MMSC and AMSC, particularly where antennas with wide beam widths are used.

The most common parameter used to describe sea condition is the significant wave height (H), defined as the average value of the peak-to-trough heights of the highest one-third of all waves. Empirically, H is related to the r.m.s. height (h_o) by:

$$H = 4h_0$$

Hence, at 1.5 GHz the smaller-scale waves can be neglected and the r.m.s. value of the sea surface slopes appear to fall between 0.04 to 0.07 in the case of wave heights less than 4 m.

Thus, with diminishing satellite elevation angle, the propagation path increases, causing a decrease of signal power at the Rx side. The noise level is initially constant; however, upon reaching some critical value of the elevation angle, sea-reflection signals appear at the Rx input, which begins to affect the C/N value. To include the effect of multipath interference caused by sea-refracted signals, the reception quality would be more properly described by the C/N plus M, where M is an interfering sea-reflected signal acting as a disturbance. Thus, sea-reflected signals differ in structure and can be divided into two categories:

1 Radio signals with the rapid continuous fluctuations of amplitudes and phases and with a possible frequency shift due to the motion of small portions of the specular cross-section relative to the source of signals (noise or diffused components).

2 Radiowaves with relatively slowly changing phase close to the phase of the basic signal and with an amplitude correlating with that of the basic signal (specular component).

Consequently, within the overall specular cross-section, an angle of arrival reflected radio signals relative to the horizontal plane may be regarded as constant and can be described by the following expression:

$$\alpha = 90^o - \gamma$$

where α = angle of radio signals arrival in accordance with Figure 1. and γ = reflection angle. The modulus of sea reflection factor for L-band signals is

within 0.8 and 0.9, which means that the amplitude of the specular reflected signal is nearly the same as that of the direct signal. As measurements have shown, the noise component depends only upon an elevation angle and a wave height. Decreasing the elevation angle and increasing the wave height result in an increase in the total amplitude of the noise, which includes the noise component. At elevation angles below 5^o, the amplitude component reaches a peak value and is no longer affected by the wave height. Now an increase of the wave height causes primarily more frequent variations in the noise component. The corresponding deviation of C.N measured in 1 kHz bandwidth amounts from 4.5 to 5 dB.

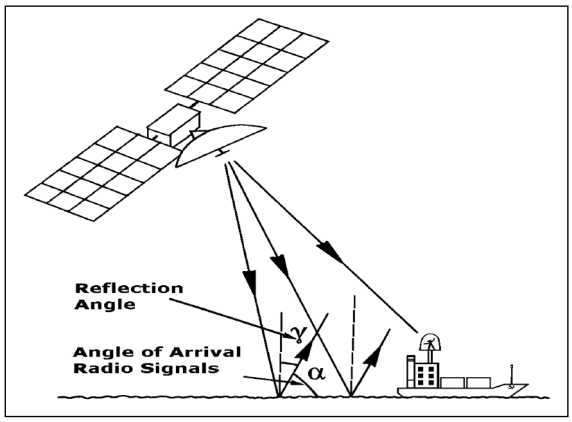

Figure 1. Geometry of Sea Reflection of Satellite Radio Signals
Courtesy of Book: "Global Mobile Satellite Communications" by D.S. Ilcev

The specular component that appears at the Rx input together with the direct signal causes fading in the direct signal due to both the minor difference between their phases and the slow change of the parameters of the reflected signals. The ratio of the direct to specular reflected signal can be described as:

$$C/M = (C + G_\varepsilon) - [C - G_{(\alpha + \varepsilon)}]$$

where C = direct signal; M = specular reflected signal power from the sea; G_ε = maximum gain of the receive SES antenna pointing towards the satellite; ε = elevation angle and α, as is shown in Figure 1. In addition, keeping accuracy sufficient for practical purposes, the previous relation gives:

$$C/M = \beta_{C/N} + [G_\varepsilon - G_{(\alpha + \varepsilon)}]$$

where $\beta_{C/N}$ = deviation of C/N ratio. With decreasing elevation angle, the C/M diminishes monotonically, except for the elevation angle range of 5^o to 8^o, within which a rise in C/N is observed. This is obviously due to the fact that at the said angles the difference in path between the direct and the specular signal becomes negligible, so that conditions appears close to the summation of the similar signals at the receiver input. An increase of the C/N plus M ratio is observed simultaneously due to reaching a peak value of amplitude in the noise (diffused) component. In fact, experimental measurements show that as the elevation angle decreases from 10^o to 1^o, the mean C/N plus M diminishes from 22–24 dB to 17–18 dB, with the deviation increasing from 1.5–2 dB to 4.5–5 dB.

4 MULTIPATH FADING CALCULATION MODEL FOR REFLECTION FROM THE SEA

The amplitude of the resultant signal at the SES terminal, being the sum of the direct wave component, the coherent and the incoherent reflection components, has a Nakagami-Rice distribution (see ITU R P.1057). The cumulative distribution of fading depends on the coherent-to-incoherent signal intensities. For example, in the case of rough sea conditions at 1.5 GHz, the coherent reflection from the sea is virtually non-existent and the coherent signal is composed only of the direct component. Therefore, the fading is determined by the Carrier-to-Multipath ratio (C/M), i.e., the power ratio of the direct signal and multipath component caused by incoherent reflection. The maximum fade depth (Φ_{max}) occurs when the coherent multipath signal is in anti-phase with the direct signal, given by:

$$\Phi_{max} = -20 \log (1 - A_r) \quad [dB]$$

where A_r = amplitude of the coherently reflected component. The value decreases rapidly with increasing wave height, elevation angle and RF. In practice, due to the vertical motion of the ship antenna relative to average sea surface height, the maximum fade value will seldom occur. By adding Φ_{max} and $\Phi_i(p)$ as signal fade due to the incoherent component in the function of time percentage (p), a practical estimate of the combined fading effects of the coherent and incoherent multipath signal for sea conditions is obtained:

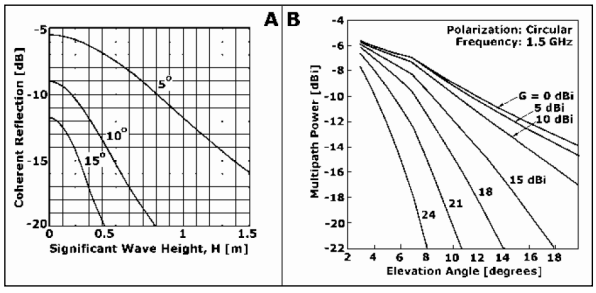

Figure 2. Estimates of Coherent Reflection and Multipath Power
Courtesy of Book: "Mobile Antenna Systems Handbook" by K. Fujimoto and J.R. James

$$\Phi_c = \Phi_{max} + \Phi_i(p)$$

The maximum fade value due to the coherent component will not occur constantly because of the vertical motion of the ship antenna relative to average sea surface height; therefore, the estimate using this equation seems to give the worst-case value. In practice, for low elevation angles (les than 10^o) at around L-band frequencies, the maximum fading occurs when the significant sea wave height is between 1.5 and 3 m, where the coherent reflected component is negligible. Accordingly, the dependence of fading depth on wave height in this range is relatively small.

The amplitude level of the coherent component decreases rapidly with increasing sea wave height, elevation angle and frequency. Figure 2. (A) illustrates the relationship between coherent reflection and significant wave height. Namely, estimates of amplitude of the coherent component for an omnidirectional antenna as a function of a significant wave height for low elevation angles are illustrated; the frequency is 1.5 GHz and polarization is circular. Thus, the incoherent component is random in both amplitude and phase, since it originates from a large number of reflecting facets on the sea's waves. The amplitude of this component follows Rayleigh distribution and the phase has a uniform distribution.

Since the theoretical model concerning the incoherent components is not suitable for engineering computations using a small calculator, simpler prediction models are useful for the approximate calculation of fading. Such simple methods for predicting multipath power or fading depth have been recently developed. Thus, in Figure 2. (B) is presented the relationship between multipath power and elevation angle for different antenna gains. Although fading depth depends slightly on sea surface conditions, even if the incoherent is dominant, the simple model is useful for a rough estimate of fading depth.

Fading depth, which is a scale of intensity of fading, is usually defined by the difference in decibels between the direct wave signal level and the signal level for 99% of the time. The fading depth can be approximated by a 50% to 99% value for fading where the incoherent component is fully developed. Large fading depths usually appear in rough sea conditions, where the incoherent component is dominant. Thus, Figure 3. (A) shows the fading depth estimated by the simple method for antenna not exceeding for 99% of the time and the corresponding C/M ratio for circular polarization at 1.5 GHz band under the condition of significant wave heights from 1.5 to 3 m. The antenna gains of 24, 20, 15 and 8 dB are functions of elevation angle with a fully-developed incoherent component. The calculation is based on the theoretical method, where the shaded area covers the practical range of the sea wave slope, which depends on fading depth in rough sea conditions. Values estimated by this simple method give the mean values of those given in Figure 3. (B).

On the other hand, as the theoretical model is not suitable for engineering computations using a small calculator, these simple prediction models are really useful for the approximate calculation of fading or interference. Such simple methods for predicting multipath power or fading depth have been developed by Sandrin and Fang [1986] and by Karasawa and Shiokawa [1988] for MMSS and Karasawa [1990] for AMSS.

Furthermore, the frequency spectral bandwidth of temporal amplitude variations enlarges with increasing wave height and elevation angle. Figure 3. (B) shows the probable range of –10 dB spectral bandwidth (which is defined by the frequency corresponding to the spectral power density of –10 dB relative to the flat portion of power spectrum) of L-band multipath fading obtained by the theoretical fading model as a function of the elevation angle under the usual conditions of MMSC; namely, significant wave height of 1 m to 5 m, ship speed of 0 to 20 knots and rolling conditions of 0 to 30^o.

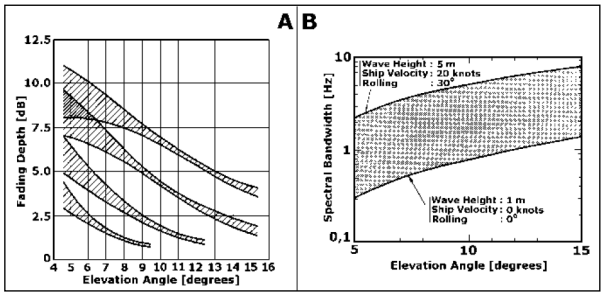

Figure 3. Estimates of Fading Depth and Spectral Bandwidth
Courtesy of Book: "Mobile Antenna Systems Handbook" by K. Fujimoto and J.R. James

5 OTHER ESTIMATIONS OF FADING FOR MMSC AND AMSC SYSTEMS

The error pattern in digital transmission systems affected by multipath fading is usually of the burst type. Accordingly, a firm understanding of the fade duration statistics of burst type fading is required. Mean value of fade duration (Φ_D) and fade occurrence interval (Φ_o) for a given threshold level as a function of time percentage, can be estimated from the fading spectrum. A simple method for predicting the mean value from the –10 dB spectral bandwidth is available as a theoretical fading model.

Predicted values of (Φ_D) and (Φ_o) for 99% of the time at an elevation angle from 5 to 10^o are 0.05 to 0.4 sec for (Φ_D) and 5 to 40 sec for (Φ_o). The probability density function of (Φ_D) and (Φ_o) at any percentages ranging from 50% to 99% approximates an exponential distribution.

1 Simple Prediction Method of Fading Depth – According to theoretical analysis and experimental results made by the mentioned researchers in Japan, the lowest elevation angle Earth-to-space path at 1.5 GHz RF band satisfies the energy conservation law: [Power of coherent component] + [Average power of incoherent component] ~ Constant. If this expression is satisfied, the maximum incoherent power can be estimated easily by calculating the coherent power at u = 0. Otherwise, for a more accurate estimation, small modifications of some parameter dependencies are necessary. The modified procedure has been adopted in P.680 for MMSC and P.682 ITU-R Recommendations for AMSC. Figure 4. (A) shows a scattergram of measured and predicted fading depths (i.e., fade for 99% of the time relative to that for 50%) in the case of MMSC systems between measured data and predicted values derived from the simple calculation method with the same conditions. In this figure, Φ_{dp2} are values from the method set out in ITU-R P.680, while Φ_{dp1} are those from an alternative procedure of the prediction method for scattering angles. It is evident that the values given by these methods agree well with the experimental values although the methods are rather approximate.

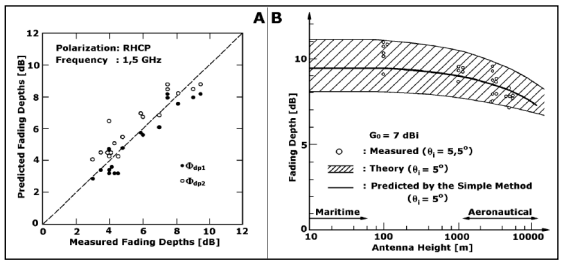

Figure 4. Scattergram and Altitude Dependence of Fading Depth Courtesy of Handbook: "Radiowave Propagation Information for Predictions for Earth-to-Space Path Communications" by ITU

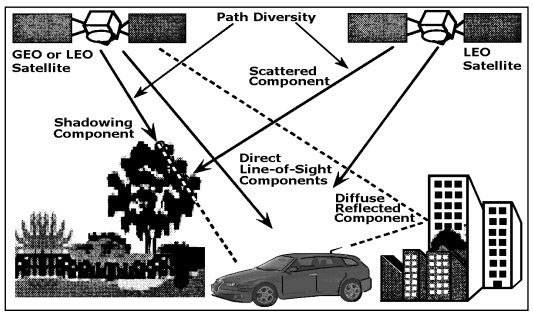

Figure 5. Typical LMSC Propagation Environment
Courtesy of Book: "Mobile Satellite Communications" by S. Ohmori and other

In Figure 4. (B) is shown the altitude dependence of signal fade depth not exceeded for 99% of the time vs. antenna height on board ships or aircraft. This experiment was obtained from measurements with a helicopter together with the calculated values from the simple estimation method of the solid line and the theoretical model of the shaded region in the figure. From the figure it can be seen that the simple prediction method agrees well with both the theoretical model and measured data even in the case of the AMSC system.

2 Fading Spectrum – In system design, particularly for digital transmission systems, it is important not only to estimate the fading depth but also to know the properties of temporal variation, such as the frequency power spectrum. For MMSC systems, theoretical analyses were carried out in Japan and all parameters affecting the spectrum such as wave height, wave direction, ship's direction and velocity, path elevation angle and antenna height variations due to ship's motion (rolling and pitching) were taken into account. In general, spectrum bandwidth is broader with increasing wave height, elevation angle, ship velocity and the relative motion of the ship borne antenna. The dependence of the spectral shape on antenna polarization and gain is usually very small. Moreover, since the speed of aircraft is significantly higher than that of ships, the fluctuation speed of multipath fading in AMSC is much faster than that in MMSC, depending on the flight elevation angle measured from the horizontal plane. The calculated –10 dB spectral bandwidth is between 20 and 200 Hz for elevation angles of 5^o to 20^o, for flight elevation angles 0^o to 5^o at a speed of 1,000 km/h.

6 FADING IN LMSC SYSTEM DUE TO SIGNAL BLOCKAGE AND SHADOWING

Recently, in the USA, Canada, Australia, Japan and Europe, domestic LMSC and GMPSC services have started. The main purpose of these systems is to extend MSC voice services to rural/remote areas where terrestrial/cellular services are not provided. In a typical urban environment, line-of-sight for cellular systems sometimes is not available due to blockage by buildings and other structures, when a MES can receive many waves reflected from these structures and conduct communication link using these signals.

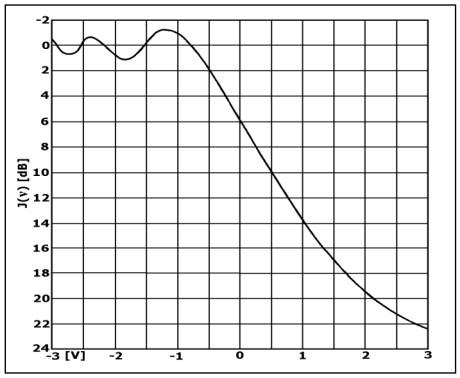

Figure 6. Loss due to Knife-Edge Diffraction
Courtesy of Handbook: "Radiowave Propagation Information for Predictions for Earth-to-Space Path Communications" by ITU

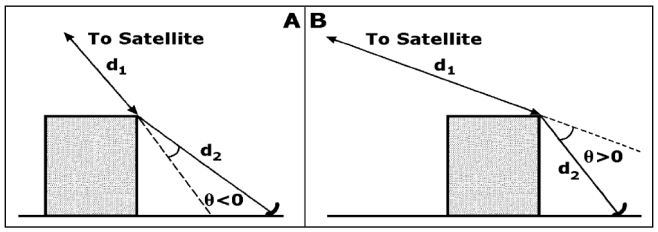

Figure 7. Geometry of Knife-edge Diffraction Phenomena
Courtesy of Handbook: "Radiowave Propagation Information for Predictions for Earth-to-Space Path Communications" by ITU

The LMSC system can be expected to use the direct line-of-sight signal from a satellite because of the high elevation angles. When the line-of-sight is blocked by any obstacle, MSC is not available, but using path diversity the link is available because of overlapping of two or more signal from adjacent satellites. At present, path diversity from separate satellites is rarely used for GEO MSS, but Non-GEO MSS have an inherent capability to exploit diversity, because the number of satellites is large providing path diversity. At this point, Figure 5. presents a typical propagation environment for scattering, multipath fading, shadowing, diffusion, ect.

Therefore, to design LMSC system, one needs information about the propagation statistics of multipath fading and shadowing. A vehicle runs at a distance of 5 to 20 m from roadside obstacles using an omnidirectional antenna, which has azimuthally uniform gain but elevation directivity, or a medium or high-gain antenna with automatic tracking capability. Thus, signal blockage and shadowing effects occur when an obstacle, such as roadside trees, overpasses, bridges, tunnels, utility poles, high buildings, hills or mountains, impedes visibility to the focus of satellite. This results in the attenuation of the received signal to such an extent that transmissions meeting a certain quality of service may not be possible. At any rate, in the shadowing environments the presence of the trees will result in the random attenuation of the strength of the direct path signal. Hence, the depth of the fade is dependent on a number of parameters including tree type, height, as well as season due to the leaf density on the trees. Whether a VES is transmitting on the left or right-hand side of the road could also have a bearing on the depth of the fade, due to the line-of-sight path length variation through the tree canopy being different for each side of the road. In fact, fades of up to 20 dB at the L-band may be presented due to shadowing caused by roadside trees. This shadowing by roadside trees cannot occur on modern highways because they are free of trees, only sometimes can shadowing appear by tunnels, very big constructions, bridges and mountains or hills in narrow passages.

1 **Tree Shadowing** – Attenuation due to trees nearby the roads arises from absorption by leaves and blockage by trunks and branches. Absorption by leaves is a function of the type and size of leaves and the water content therein. Blockage due to trunks is primarily a function of their size. In addition to attenuation of the direct signal, trees also cause an incoherent component due to signals reflected and diffracted off the tree surfaces.
The overall attenuation from different types of fully foliated trees varies from 10.6 to 14.3 dB and the attenuation coefficient is from 1.3 to 1.8 dB/m. Measurements were conducted with MES Rx in a rural environment. Based on these average values, a frequency scaling law for the attenuation coefficient has been derived [Goldhirsh and Vogel] by:

$$a_1 = a_0 \sqrt{f_1/f_0} \quad [\text{dB/m}]$$

where a_1 and a_0 = attenuation coefficients at frequencies f_1 and f_0 [GHz], respectively. Hence, the range of variation for a_1 at 1.5 GHz is from 0.5 to 1.7 dB/m. Moreover, trees without foliage attenuate less and the reduction in attenuation appears to be proportional to the total attenuation experienced when the tree is fully foliated. The received strength of the direct signal behind a tree will depend on the orientation of the signal path with respect to the tree. The amount of absorbing matter lying along the path will determine the degree of attenuation and hence, on average, the length of the signal path through the tree shield can be considered a major factor in determining the signal level. The path length is a function of the elevation angle and the distance between the receiver and the tree. At this point, the average attenuation behind an isolated tree can be estimated as the product of the attenuation coefficient and the path length through the tree. The path length through the tree canopy will depend on its shape and the orientation of the signal path within the canopy. Depending on the type being considered, the tree canopy may be modeled as any one of the shapes.

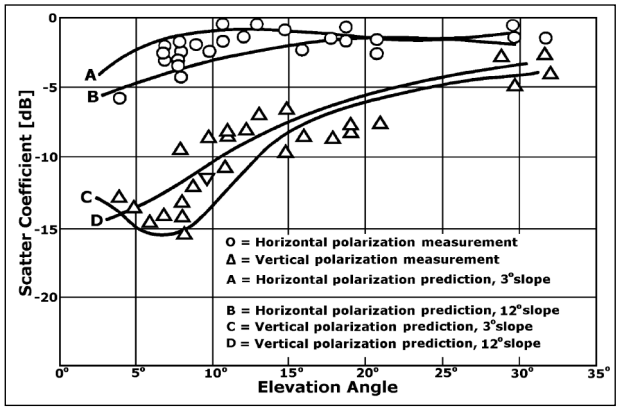

Figure 8. Ocean Mean-Square Scatter Coefficients vs. Elevation
Courtesy of Handbook: "Radiowave Propagation Information for Predictions for Earth-to-Space Path Communications" by ITU

For the intermediate elevation angle (20^o to 50^o), attenuation is almost independent of elevation and dependence becomes important only at the higher and lower ends of the elevation angle range. By considering the path length variability as a statistical parameter, however, a tree can be modeled as giving an average attenuation and a distribution around it. Both the coherent and incoherent components will vary with the receiver position and complete decorrelation of the signal is expected over distances in the order of a few wavelengths.

2 Building Shadowing – Signal reception behind buildings takes place mainly through diffraction and reflection. A direct line-of-sight component does not usually exist and therefore shadowing cannot be defined unambiguously, as in the case of trees. However, shadowing may be loosely defined as the power ratio between the average signal levels to the unscheduled direct signal level. Otherwise, diffractions from buildings can be studied using knife-edge diffraction theory, which gives reasonable estimates. A concept view of knife-edge diffraction phenomena is shown in Figure 6. for all losses caused by the presence of the obstacles as a function of a dimensionless parameter ν and in Figure 7., which illustrates the geometry of the path for both the illuminated (A) and shadowed cases (B), in order to calculate the parameter ν, by using elevation and wavelength as follows:

$\nu = \varepsilon \sqrt{2/[\lambda(1/d_1 + 1/d_2)]}$ but $d_1 >> d_2$, so: $\nu = \varepsilon \sqrt{2}/\lambda\ (1/d_2) = \varepsilon \sqrt{2d_2/\lambda}$

The signal strength at the shadow boundary is 6 dB below the line-of-sight level. In the illuminated region, the signal fluctuations are experienced due to interference between the direct and the diffracted components. Hence, once inside the shadowed region, the shadow increases rapidly. An experimental investigation into building shadowing loss conducted by Yoshikawa and Kagohara in 1989 confirmed the applicability of the knife-edge diffraction theory. Measured signal strength behind a building at various distances was found to follow the prediction made, assuming a single diffraction edge. However, where the building is narrow compared with its height, there may be significantly less shadowing than predicted by the above procedure. When the direct signal path is blocked by a building, diffractions of the buildings are not expected to play a dominant role in establishing the communication link, unless MES is close to the shadow boundary. Reflections may play a useful role in such situations, as happens in cellular systems. Building penetration depends on the type of exterior material of the building and the location inside the building. Thus, the loss through the outer structure, known as the penetration loss, is defined as the difference in median signal levels between that measured immediately outside the building at 1.5 m above the ground and that immediately inside the buildings at some reference level on the floor of interest.

Measurements made at 940 MHz in a medium-size city in the USA indicate that on the ground floor of typical steel-concrete-stone office buildings, the average penetration is about 10 dB with a standard deviation of about 7 dB. While another set of measurements in a large city resulted in average ground floor penetration loss of 18 dB with a standard deviation of 7.7 dB. However, the overall decrease of penetration loss with height was about 1.9 dB per floor. The biggest average attenuations are 12 dB and 7 dB and standard deviations are 4 db and 1 dB for metal and concrete, respectively.

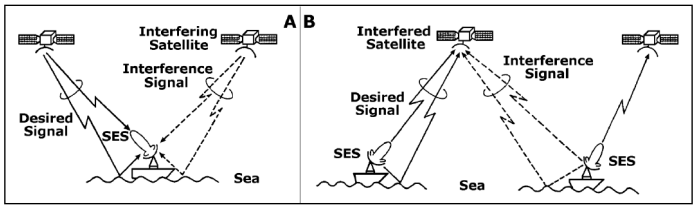

Figure 9. Basic Model for Intersatellite Interferences Phenomena
Courtesy of Handbook: "Radiowave Propagation Information for Predictions for Earth-to-Space Path Communications" by ITU

Attenuation through glass ranges from about 2 to 6 dB depending on the type of glass, i.e., plain glass produces less attenuation compared to tinted or coated glass, containing metallic components. Otherwise, the smallest average attenuation is through office furnishings, aluminum and wood/brick of about 1, 2 and 3 dB, respectively. Losses within a building are both of distance from the exterior wall blocking the signal path, as well as the interior layout. Measurements have resulted in an inverse distance power

law coefficient ranging from 2 to 4. The forthcoming ICO system has conducted experiments with satellite-borne signals whose final target is to improve and even to eliminate building shadowing.

7 FADING IN AMSC SYSTEM DUE TO LAND REFLECTION

An experiment aboard a helicopter over land was carried out by receiving right-hand circularly polarized 1.5 GHz beacon signals from an IOR Marisat satellite at an elevation angle of 10^o. Fading depths measured over plains such as paddy fields were fairly large (about 5 dB), nearly equal to that for sea reflection. However, fade depths measured over mountainous and urban areas were less than 2 dB. In the case of mountains, reflected waves are more likely to be shadowed or diffused by the mountains. As to urban areas, the shadowing and diffusing effects of reflected wave by buildings are also large. For this reason, the ground reflected multipath fading in these cases is not generally significant.

Measurements of Sea-Reflection Multipath Effect – A study of multipath propagation at 1.5 GHz was performed with KC-135 aircraft and the NASA ATS-6 satellite. Otherwise, the signal characteristics were measured with a two-element waveguide array in the aircraft noise radome, with 1 dB beam width of 20^o in azimuth and 50^o in elevation. Namely, data was collected over the ocean and over land at a normal aircraft altitude of 9.1 km and with a nominal speed of 740 km/h. Coefficients for horizontal and vertical antenna polarization were measured in an ATS-6 experiment, where values for r.m.s. sea surface slopes of 3o and 12o were plotted versus elevation angle, in Figure 8., along with predictions derived from a physical optics model. Sea slope was found to have a minor effect for elevation angles above about 10^o. The agreement between measured coefficients and those predicted for a smooth flat Earth as modified by the spherical Earth divergence factor increased as sea slope decreased.

The relationship between r.m.s. sea surface and wave height is complex but conversion can be performed. Namely, for most aeronautical systems, circular polarization will be of greater interest than linear. For the simplified case of reflection from a smooth Earth, which should be a good assumption for elevation angles above 10^o, circular co-polar and cross-polar scatter coefficients (S_c and S_x), respectively, can be expressed in terms of the horizontal and vertical coefficients (S_h and S_v), respectively by:

$$S_c = (S_h + S_v)/2 \quad \text{and} \quad S_x + (S_h - S_v)/2$$

For either incident RHCP or LHCP is employed. Thus in general, the horizontal and vertical coefficients are complex values and phase information is required to apply the last equitations to the curve, in Figure 8.

8 INTERFERENCE FROM ADJACENT SATELLITE SYSTEMS

In GMSC systems for ships, vehicles and aircraft, small mobile antennas are essential for operational and economic reasons. As a result, a number of low G/T value MES terminals with smaller antennas have been developed. However, such antenna systems are subject to the restriction of frequency utilization efficiency, or coexistence between two or more satellite systems in the same frequency band and/or an overlap area where both satellites are visible.

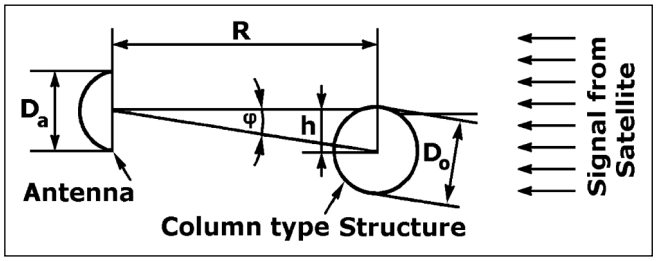

Figure 10. Geometry of Blocking
Courtesy of Handbook: "Radiowave Propagation Information for Predictions for Earth-to-Space Path Communications" by ITU

For coordination between two different systems in the same frequency band, a highly reliable interference evaluation model covering both interfering and interfered with conditions is required. Investigation into this area has been undertaken in particular by ITU-R Study Group 8. Advancement of such a model is an urgent matter for the ITU-R considering the number of MSC systems that are being developed in the meantime.

In GMSC systems, the desired signal from the satellite and the interfering signal from an adjacent satellite independently experience amplitude fluctuations due to multipath fading, necessitating a different treatment from that for fixed satellite systems. The main technical requirement is a formulation for the statistics of differential fading, which is the difference between the amplitude of the two satellite signals. At this point, the method given in No 5 of ITU-R P.680 Recommendation therefore presents a practical prediction method for signal-to-interference ratio where the effect of thermal noise and noise-like interference is taken into account; assuming that the amplitudes of both the desired and interference signal affected by the sea reflected multipath fading follow Nakagami–Rice distributions. In

fact, this situation is quite probable in MMSC systems.

The basic assumptions of the intersatellite model are shown in Figure 9., as an example of interference between adjacent satellite systems, where (A) is downlink interference on the MES side and (B) is uplink interference on the satellite side. This applies to multiple systems sharing the same frequency band. It is anticipated that the interference causes an especially severe problem when the interfering satellite is at a low elevation angle viewed from the ship presented in this figure because the maximum level of interference signal suffered from multipath fading increases with decreasing elevation angle. Another situation is interference between beams in multi-spot-beam operation, where the same frequency is repeatedly allocated.

9 SPECIFIC LOCAL ENVIRONMENTAL INFLUENCE IN MMSC

Local environmental influence is important for SES equipped with beam width antenna. Many factors, with different kinds of noise sources, tend to make disturbances in MMSC channels. Another factor that affects communication links is RF emission from different noise sources in the local environment. Specific local ship environmental factors can be noise contributions from various sources in the vicinity of the SES and the influence of the ship's superstructure in the operation of maritime mobile terminals. However, some of these local environmental factors can affect SES when a ship is passing nearby the coast and, some of these are permanent noise sources. More exactly, these environmental sources include broadband noise sources, such as electrical equipment and motor vehicles and out-of-band emission from powerful transmitters such as radars and ships HF transmitters.

9.1 *Noise Contribution of Local Ships' Environment*

Some of the noise contributions from the local ships' environment are as follows:

1 Atmospheric Noise from Absorption – Absorbing atmospheric media, such as water vapor, precipitation particles and oxygen emit thermal noise that can be described in terms of antenna noise temperature. These effects were discussed at the beginning of this chapter.
2 Industrial Noise – Heavy electrical equipment tends to generate broadband noise that can interfere with sensitive receivers. Therefore, a high percentage of this noise originates as broadband impulsive noise from ignition circuits. Namely, the noise varies in magnitude by as much as 20 dB, depending on whether it is measured on a normal working day or on weekends and holidays when it is lower in magnitude.
3 Out of Band Emission from Radar – Ship borne and surveillance radars operating in pulse mode can generate out of band emission that can interfere with SES receivers. In general, such emissions can be suppressed by inserting waveguide or coaxial filters at the radar transmitter output.

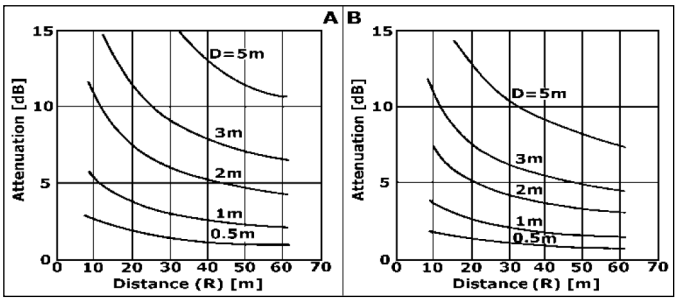

Figure 11. Estimated Attenuation due to Blocking
Courtesy of Handbook: "Radiowave Propagation Information for Predictions for Earth-to-Space Path Communications" by ITU

4 Interference from High Power Communication Transmitters – High power ships and terrestrial transmitters, for example HF ship radio transceivers; HF radio diffusion and TV broadcasting can interfere with SES.
5 Interference from Vehicles – Under certain operational conditions, RF emissions from vehicles may impair Rx sensitivity. Accordingly, in one measurement the noise emanating from heavy traffic has to be about –150dB (mW/Hz) within the frequency band 1.535 to 1.660 MHz.
6 Shipyard Noise – Extremely high peak amplitudes of noise of –141 dB (mW/Hz) were recorded from Boston Navy Yard, which was in full operation at that time. Thus, this noise is also a combination of city ambient noise and broadband electromagnetic noise from industrial equipment.

9.2 *Blockages Caused by Ship Superstructures*

Ship's superstructures can produce both reflection multipath and blockage in the direction of the satellite. For the most part, reflections from the ship's superstructure located on the deck can be considered coherent with the direct signal. The fading depth due to these reflections depends on a number of construction parameters including shape of the ship, location of the ship's antenna, antenna directivity and sidelobe level, axial ratio and orientation of the polarization ellipse, azimuth and elevation angles towards the satellite, etc. Antenna gain has a significant influence on the fading depth. In this case, low gain antennas with broader beam widths will collect

more of the reflected radio signals, producing deeper fades.

Blockage is caused by ship superstructures, such as the mast and various types of antennas deployed on the ship. The geometry of blockage by a mast is presented in Figure 10. Signal attenuation depends on several parameters including diameter of column, size of antenna and distance between antenna and column. Accordingly, estimated attenuation due to blocking by a column type structure is shown in Figure 11 for antenna gains of 20 dB (A) and 14 dB (B), respectively.

9.3 *Motion of Ship's Antenna*

The motion of mobile satellite antennas is an important consideration in the design of MMSC systems. The received signal level is affected by the antenna off-beam gain because the antenna motion is influenced by the ship's motion. The random ship motion must be compensated by a suitable stabilizing mechanism to keep the antenna properly pointed towards the satellite. This is normally achieved either through a passive gravity stabilized platform or an active antenna tracking system. In either case, the residual antenna pointing error can be significant enough to warrant its inclusion in the overall link calculation.

Earlier experimental evidence suggests that the roll motion of a ship follows a zero mean Gaussian distribution over the short-term of the sea waves. The standard deviation of the distribution (σ_s) is a function of the vessel characteristics and the sea state of the wave height. In Figure 12 is illustrated the distribution of the instantaneous roll angle of a ship under moderate to rough sea conditions. The distribution of the ship motion approximates to a Gaussian standard deviation of distribution with σ_s = 5.42 value.

Also shown in the figure is the distribution of roll angle of a passively stabilized antenna under the same conditions, which also follows a zero mean Gaussian distribution with a quantum of σs = 0.99. Solid curves in Figure 5.17. represent measured values and dashed curves show calculated values for stabilized antenna motion over the sea conditions with wave heights of approximately 5 m.

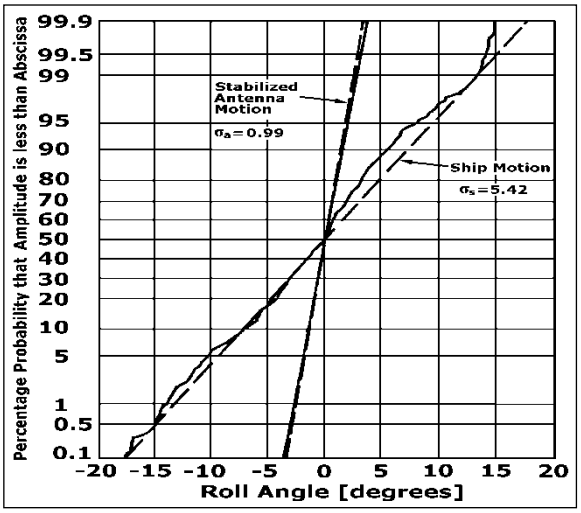

Figure 12. Measured Stabilized Antenna Motion
Courtesy of Handbook: "Radiowave Propagation Information for Predictions for Earth-to-Space Path Communications" by ITU

Otherwise, the relation between the standard deviations of the two distributions depends on the design of the passive stabilizer. Although the ship's antenna motion is much reduced, depending on the antenna beam width, the residual pointing error may be large enough to produce appreciable signal fluctuations. Over a long period of sea waves time σs varies as a function of the sea surface conditions and its distribution can be approximately by either a log normal distribution or a Weibull distribution.

10 CONCLUSION

The common satellite channel environment affects radiowave propagation in changeless ways. The different parameters influenced are mainly path attenuation, polarization and noise. The factors to be considered are gaseous absorption in the atmosphere, absorption and scattering by clouds, fog, all precipitation, atmospheric turbulence and ionospheric effects. In this sense, several measurement techniques serve to quantify these effects in order to improve reliability in the system design. Because these factors are random events, GMSC system designers usually use a statistical process in modeling their effects on radiowave propagation. To design an effective GMSC model it is necessary to consider the quantum of all propagation characteristics, such as signal lost in normal environment, path depolarization causes, transionospheric contribution, propagation effects important for mobile systems, including reflection from the Earth's surface, fading due to sea and land reflection, signal blockage and to the different local environmental interferences for all mobile and handheld applications. At any rate, the local propagation characteristics on the determinate geo-

graphical position have very specific statistical proprieties and results for ships, vehicles and aircraft.

REFERENCES

[01] Evans B.G., "Satellite communication systems", IEE, London, 1991.

[02] Freeman R.L., "Radio systems design for telecommunications (1-100 GHz)", John Wiley, Chichester, 1987.

[03] Fujimoto K. & other, "Mobile antenna systems handbook", Artech House, London, 1994.

[04] Galic R., "Telekomunikacije satelitima", Skolska knjiga, Zagreb, 1983.

[05] Group of authors, "Handbook - Mobile Satellite Service (MSS)", ITU, Geneva, 2002.

[06] Group of authors, "Handbook on Satellite Communications", ITU, Geneva, 2002.

[07] Group of authors, "Morskaya radiosyaz", Transport, Leningrad, 1985.

[08] Group of authors, "Radiowave propagation information for predictions for earth-to-space path communications", ITU, Geneva, 1996.

[09 Ilcev D. St. "Global Mobile Satellite Communications for Maritime, Land and Aeronautical Applications", Book, Springer, Boston, 2005.

[10] Maral G. & other, "Satellite communications systems", John Wiley, Chichester, 1994.

[11] Novik L.I. & other, "Sputnikovaya svyaz na more", Sudostroenie, Leningrad, 1987.

[12] Ohmori S. & other, "Mobile satellite communications", Artech House, Boston–London, 1998.

[13] Richharia M., "Mobile Satellite Communications – Principles and Trends", Addison-Wesley, Harlow, 2001.

[14] Sheriff R.E. & other, "Mobile satellite communication networks", Wiley, Chichester, 2001.

[15] Zhilin V.A., "Mezhdunarodnaya sputnikova sistema morskoy svyazi – Inmarsat", Sudostroenie, Leningrad, 1988